NASA-CR-167535
ED 6

1. Kumar Krishen

7. ARL-TR-81-41

Copy No. 2

2. MATHEMATICAL MODELING AND SAR SIMULATION MULTIFUNCTION SAR TECHNOLOGY EFFORTS

Final Report under Contract NAS9-16171

3. Carroll R. Griffin
James M. Estes

4. APPLIED RESEARCH LABORATORIES
THE UNIVERSITY OF TEXAS AT AUSTIN
POST OFFICE BOX 8029, AUSTIN, TEXAS 78712

5. NAS9-16171

6. 10 September 1981

Final Report

1 August 1980 - 31 July 1981

Prepared for:

NATIONAL AERONAUTICS AND SPACE ADMINISTRATION
LYNDON B. JOHNSON SPACE CENTER
HOUSTON, TX 77058

UNCLASSIFIED

SECURITY CLASSIFICATION OF THIS PAGE (When Data Entered)

REPORT DOCUMENTATION PAGE

READ INSTRUCTIONS BEFORE COMPLETING FORM

1. REPORT NUMBER	2. GOVT ACCESSION NO.	3. RECIPIENT'S CATALOG NUMBER
4. TITLE (and Subtitle) MATHEMATICAL MODELING AND SAR SIMULATION MULTIFUNCTION SAR TECHNOLOGY EFFORTS		5. TYPE OF REPORT & PERIOD COVERED final report 1 August 1980 - 31 July 1981
		6. PERFORMING ORG. REPORT NUMBER ARL-TR-81-41
7. AUTHOR(s) Carroll R. Griffin James M. Estes		8. CONTRACT OR GRANT NUMBER(s) NAS9-16171
9. PERFORMING ORGANIZATION NAME AND ADDRESS Applied Research Laboratories The University of Texas at Austin Austin, Texas 78712		10. PROGRAM ELEMENT, PROJECT, TASK AREA & WORK UNIT NUMBERS
11. CONTROLLING OFFICE NAME AND ADDRESS National Aeronautics and Space Administration Lyndon B. Johnson Space Center Houston, TX 77058		12. REPORT DATE 10 September 1981
		13. NUMBER OF PAGES 57
14. MONITORING AGENCY NAME & ADDRESS(if different from Controlling Office)		15. SECURITY CLASS. (of this report) UNCLASSIFIED
		15a. DECLASSIFICATION/DOWNGRADING SCHEDULE

16. DISTRIBUTION STATEMENT (of this Report)

17. DISTRIBUTION STATEMENT (of the abstract entered in Block 20, if different from Report)

18. SUPPLEMENTARY NOTES

19. KEY WORDS (Continue on reverse side if necessary and identify by block number)

synthetic aperture radar
orbiting platform SAR
simulation

20. ABSTRACT (Continue on reverse side if necessary and identify by block number)

The orbital SAR (synthetic aperture radar) simulation program (OSS) developed by ARL:UT was used in several simulation efforts directed toward advanced SAR development. This report details efforts toward simulating a new operational radar designed by the NASA Jet Propulsion Lab, simulation of antenna polarization effects, and simulation of SAR images at several different wavelengths. Avenues for improvements in the OSS and its application to the development of advanced digital radar data processing schemes are indicated.

DD FORM 1473, 1 JAN 73 EDITION OF 1 NOV 65 IS OBSOLETE

UNCLASSIFIED

SECURITY CLASSIFICATION OF THIS PAGE (When Data Entered)

PRECEDING PAGE BLANK NOT FILMED

TABLE OF CONTENTS

LIST OF FIGURES

PRECEDING PAGE BLANK NOT FILMED

LIST OF TABLES

I. INTRODUCTION

The contract was initially oriented toward simulating the radar parameters of the ASAR (Advanced Synthetic Aperture Radar) system under development jointly by NASA/JPL and NASA/JSC. The former had been tasked to develop a system using a technique known as "burst mode" with wavelength diversity in pulse bursts of transmissions. NASA/JSC was responsible for developing the antenna system required for handling the wide band of frequencies involved. The ARL:UT supporting effort was to simulate the system design and particularly the "burst mode", to provide insight into the operation of the algorithms and anticipated results. The simulation developed by ARL:UT for an orbiting SAR platform had to be modified to support the aircraft based ASAR.

After three months of effort toward these objectives, a decision was made to stop further work on the ASAR system and instead concentrate on certain key SAR technology areas. Among these are multipolarization antennas, multifrequency radar, multibeam squint mode SAR (wide swath), calibration techniques, and burst mode implementation. Of these, ARL:UT addressed the first three in varying degree.

PRECEDING PAGE BLANK NOT FILMED

II. ASAR SIMULATION EFFORTS

A. Discussion

The ARL:UT orbital SAR simulation (OSS) had to be modified to simulate an aircraft flying in earth's atmosphere at a relatively low velocity and altitude compared to the orbiting platform. In addition, the radar parameters had to be obtained from the system designers at NASA/JPL and the antenna parameters from the project personnel at NASA/JSC. The system was to have exhibited two unique design features: extremely broad wavelength coverage, and data processing of synthetic data arrays formed by bursts of pulses at several different radar frequencies.

The purposes of the simulation were to investigate and demonstrate the validity of the system design, in particular the so-called "burst mode" operation.

Two sets of problems were encountered in this effort. The first had to do with adapting the existing simulation, of a space-based orbiting radar, to the aircraft-based design. This problem set was rather easily solved, but attempts to define the design parameters of the radar system were relatively unsuccessful initially, and two or three months elapsed before a preliminary set of parameters for use in the simulation was agreed upon and obtained.

B. Dynamics Simulation

In order to utilize the existing routines in the simulation, the proposed aircraft platform (a CV 990) was considered like an orbiting platform in a low earth gravity environment, so that it could maintain orbit at its usual altitude and velocity. The magnitude of the velocity vector is

$$V_s = a(1-e^2\cos^2E)^{1/2} \cdot \dot{E} \quad , \qquad (1)$$

with the altitude specified by the orbit radius from earth's center

$$r_s = a(1 - e \cos E) \quad . \qquad (2)$$

The gravitational constant of earth μ_p has been measured at 398,601 km^3/sec^2. In Eq. (2) e is the eccentricity of the orbit, and E is the eccentric anomaly. If e is zero, the orbit is circular. The parameter a is the semimajor axis of the orbit ellipse, or the radius of the orbit with e=0.

By selecting the proper values for the six Kepler orbital elements, a, e, i, Ω, ω, and T_p, the orbit is specified. In Eq. (1), $\dot{E}$ is the time derivative of the eccentric anomaly:

$$E - e \sin E = \nu(t-T_p) \qquad (3)$$

$$\frac{dE}{dt}(1 - e \cos E) = \nu \quad . \qquad (4)$$

Here ν is the mean angular velocity of the platform

$$\nu = \sqrt{\mu_p/a^3} \quad . \qquad (5)$$

In order to derive a usable value of μ_p we can simplify the operation by assuming a spherical earth and a circular orbit for the aircraft. We find that

$$r_s = a \quad , \quad V_s = a \times \dot{E} \quad , \quad \dot{E} = \nu \quad ; \qquad (6)$$

therefore

$$V_s = r_s \nu = a\left(\mu_p/a^3\right)^{1/2} = \left(\mu_p/a\right)^{1/2} \quad . \tag{7}$$

Assuming that the CV 990 will fly at 400 kt TAS (205 m/sec) at an altitude of 12,000 m (39,372 ft), we can solve for an imaginary value of μ_p which will provide the proper angular rate.

$$\mu_p = aV_s^2 \tag{8}$$

$$= (0.205)^2 \ (12+6378.167)$$

$$= 268.2 \ \mathrm{km}^3/\mathrm{sec}^2 \quad ,$$

compared with the measured value for earth of

$$\mu_p = 398{,}601 \ \mathrm{km}^3/\mathrm{sec}^2$$

All other planet earth parameters remain the same.

For the orbit specification, all parameters used for SEASAT, for example, can remain the same except the semimajor axis a, which becomes 6390.167 km (12+6378.167) and the orbit rotational rate η, which becomes

$$\frac{1}{2\pi}\frac{V_s}{r_s} = \frac{1}{2\pi}\left(\frac{0.205}{6390.167}\right) = 18.4 \times 10^{-4} \ \mathrm{deg/sec}$$

C. Radar Simulation

The proposed ASAR design was to have used linear FM (chirp) pulse compression, whereas the OSS is designed for binary phase coded pulse compression, which is particularly adapted to digital processing.

Some effort was spent in analyzing the pulse compression routine requirements to provide an analogous digital signal sampled at the Nyquist rate.

Following a specification review at JSC, a first attempt was made to assign radar specification values for the simulation. Table I contains most of these values.

The linear FM chirp modulation proposed for the ASAR has the following parameters.

$$f_o = 10^9 \text{ Hz} \quad ; \quad f_1 = 1.02 \times 10^9 \text{ Hz} \quad , \quad \frac{df}{dt} = 10^{12} \text{ Hz/sec}^2$$

$$T = 20 \times 10^{-6} \text{ sec} \quad .$$

The equation for the phase as a function of time is

$$\phi = \phi_o + f_o t + \frac{1}{2}\frac{df}{dt} t^2 \quad , \quad \phi_o = 0 \text{ rad} \tag{9}$$

$$\text{at} \quad t = 0 \quad , \quad \phi = \phi_o = 0$$

$$\text{at} \quad t = n \quad , \quad \phi_n = \phi_o + f_o(n) + \frac{1}{2}\frac{df}{dt} (n)^2$$

$$\text{at} \quad t = n-1 \ , \quad \phi_{n-1} = \phi_o + f_o(n-1) + \frac{1}{2}\frac{df}{dt} (n-1)^2 \quad .$$

$$\text{If } \Delta t = n - (n-1) = 1 \quad , \quad \Delta\phi = \phi_n - \phi_{n-1} = f_o + \frac{1}{2}\frac{df}{dt} (2n-1) \quad .$$

From the sampling theorem, sampling period = 1/2 period of highest frequency,

$$\text{let } \Delta t = \frac{1}{2f_1} [n-(n-1)] = \frac{1}{2f_1} = \frac{1}{2.04 \times 10^9 \text{ Hz}} = 0.49 \text{ nsec} \quad , \tag{10}$$

then

$$\phi_n = \phi_o + n\Delta t f_o + \frac{1}{2}\frac{df}{dt} (n\Delta t)^2 \tag{11}$$

$$\phi_{n-1} = \phi_o + (n-1)\Delta t f_o + \frac{1}{2}\frac{df}{dt} (n-1)^2 \Delta t^2 \tag{12}$$

TABLE I

<u>Radar Specifications</u> Radar ID: ASAR 1

Symbol	Code	Description	Value
λ	WL	Radar wavelength, m	L: 0.23513; S: 0.093685; C: 0.062457; X: 0.03[illegible]
TB	TBW	Range time-bandwidth product	400
	S/N	Received signal-to-noise ratio, dB	7.0
N_p	LRC	Sample length of range correlation	40,800
n_s	LPI	Sample length across phase interval	1
ρ_r	RESR	Ground range resolution, m	$25\sqrt{2}$
ρ_a	RESA	Azimuth resolution, m	2
s_r	SRR	Range sampling ratio	1
	KPC	Phase code, $\phi_n = 10^{-3}\pi\left[0.98 + (2n-1)\, 0.24 \times 10^{-3}\right]$ rad	
	KPCS	Phase code sequence, BCD	1
s_a	SRA	Azimuth sampling ratio	1
*	KRFTNR	Name of range impulse response function, BCD:	cosine^2
*	KWTFTNA	Name of aperture weighting function, BCD	Taylor
*	SHADFAC	Aperture weight factor	−30 dB
POR	PCOFFR	Patch-to-patch offset, range, m	0
POA	PCOFFA	Patch-to-patch offset, azimuth, m	0
SW	SW	Swath width, km	20
	NA	Number of patches	1
LAT_p	STLAT	Map start latitude, rad	$2\pi/10$
r_t	TCR	Planetocentric distance to terrain center, km	$0.63675192370 \times 10^4$
LT_t	TCLAT	Terrain center latitude, rad	$2\pi/10$
LN_t	TCLONG	Terrain center longitude, rad	π

$$\Delta\phi_n = \phi_n - \phi_{n-1} = \Delta t f_o + \frac{1}{2}\frac{df}{dt}\left[(n\Delta t^2) - (n\Delta t)^2 + (2n-1)\Delta t^2\right]$$

$$= \Delta t f_o + \frac{1}{2}\frac{df}{dt}(2n-1)\Delta t^2 \text{ cycles}$$

$$= 2\pi f_o \Delta t + \pi\frac{df}{dt}(2n-1)\Delta t^2 \text{ rad}$$

$$= 2\pi(10^6)\left(0.49\times10^{-9}\right) + \pi\frac{20\times10^6}{20\times10^{-6}}(2n-1)\left(0.49\times10^{-9}\right)^2$$

$$= 10^{-3}\pi\left[0.98 + (2n-1)\left(0.24\ 10^{-3}\right)\right]\text{rad}$$

$$= 0.18\ [0.98 + (2n-1)(0.00024)] \text{ deg} \qquad (13)$$

and

$$N_p = \frac{T}{\Delta t} = (2.04\times10^9)(20\times10^{-6}) = 40{,}800 \text{ samples.}$$

D. Antenna Simulation

The antenna design was the responsibility of JSC. It posed a special problem because a single antenna for the 10 GHz bandwidth (2-12 GHz) would be very difficult to design and build. Secondly, its design largely depended on the JPL radar design, which was not finalized. Table II gives the parameters that were selected for use in the absence of any real antenna characteristics.

E. Terrain Specifications

The terrain to be used initially was to be a model terrain used in previous work, called SINGLESCAT. It contains two discrete scatterers and a single homogeneous field. Table III describes the parameters for this model.

TABLE II

ANTENNA SPECIFICATIONS

*		KANT	Antenna identification, BCD	UNITPAT
*	n_B	SNAC	Boresight nadir at map start, rad	20°,$\pi/9$
*	ϕ_B	SQUINT	Boresight squint at map start, rad	90°,$\pi/2$
*	ϕ_{az}	ABW	Antenna azimuth angular coverage, rad	π
*	n_{el}	EBW	Antenna elevation angular coverage, rad	π
*		PHCPB(3)	Phase center position, body axis xyz, m	0,0,0
*		ABRPY(3)	Antenna attitude, body axis rpy, rad	$0,-\frac{7\pi}{18},\frac{\pi}{4}$
*		PDRPY(3)	Platform attitude rates, local orbital rpy, rad/sec	0,0,0

TABLE III

TERRAIN SPECIFICATIONS

KSNO	Terrain identification, BCD	SINGLESCAT
NDISC	Number of discretes in terrain model	2
NFLDS	Number of fields in terrain model	1
NSCATS	Total number of scatterers in terrain model	102
EMEAN	Mean echo strength	0.1
DISTAX	x-axis coverage, km	10
DISTY	y-axis coverage, km	10

A meeting was held at NASA/JPL in the third month of the contract, attended by representatives from ARL:UT and Environmental Research Institute of Michigan (ERIM), to evaluate the design objectives and status of the ASAR. The project had schedule and funding difficulties and, subsequently, NASA decided to cancel the entire project. Unfortunately, a substantial portion of the contract resources at ARL:UT had already been expended on the effort, and a simulation had not been run.

The project was reoriented with specific emphasis on three areas: antenna polarization effects, wavelength diversity effects, and implementation of a so-called "burst mode" wavelength diversity concept on a patch-by-patch basis.

III. OTHER SIMULATION INVESTIGATIONS

Figure 1 illustrates the architecture of the OSS simulation. Each intermediate step results in data on tape or disk bulk storage, which permits incremental completion of the entire simulated radar image. For the polarization and wavelength diversity experiments an existing terrain model was utilized, illustrated in Fig. 2. This figure illustrates the scene content of the test terrain as well as images derived from it.

A. Antenna Polarization Effect

A complete simulation would include the polarization sensitivity of individual scatterers and would incorporate the randomly polarized backscattering from the individual scatterers in fields of scatterers, particularly homogeneous fields. The general situation is that the backscattered wave is partially polarized, part of it completely polarized, and part of it unpolarized. Suppose we designate the degree of polarization as the ratio of the polarized power to the total power (following Kraus), or:

$$d = \frac{\text{polarized power}}{\text{total power}} , \qquad (15)$$

and denoting the Stokes parameters as s_o, s_1, s_2, s_3,

$$d = \frac{\sqrt{s_1^2 + s_2^2 + s_3^2}}{s_o} \quad 0 \leq d \leq 1 \quad . \qquad (16)$$

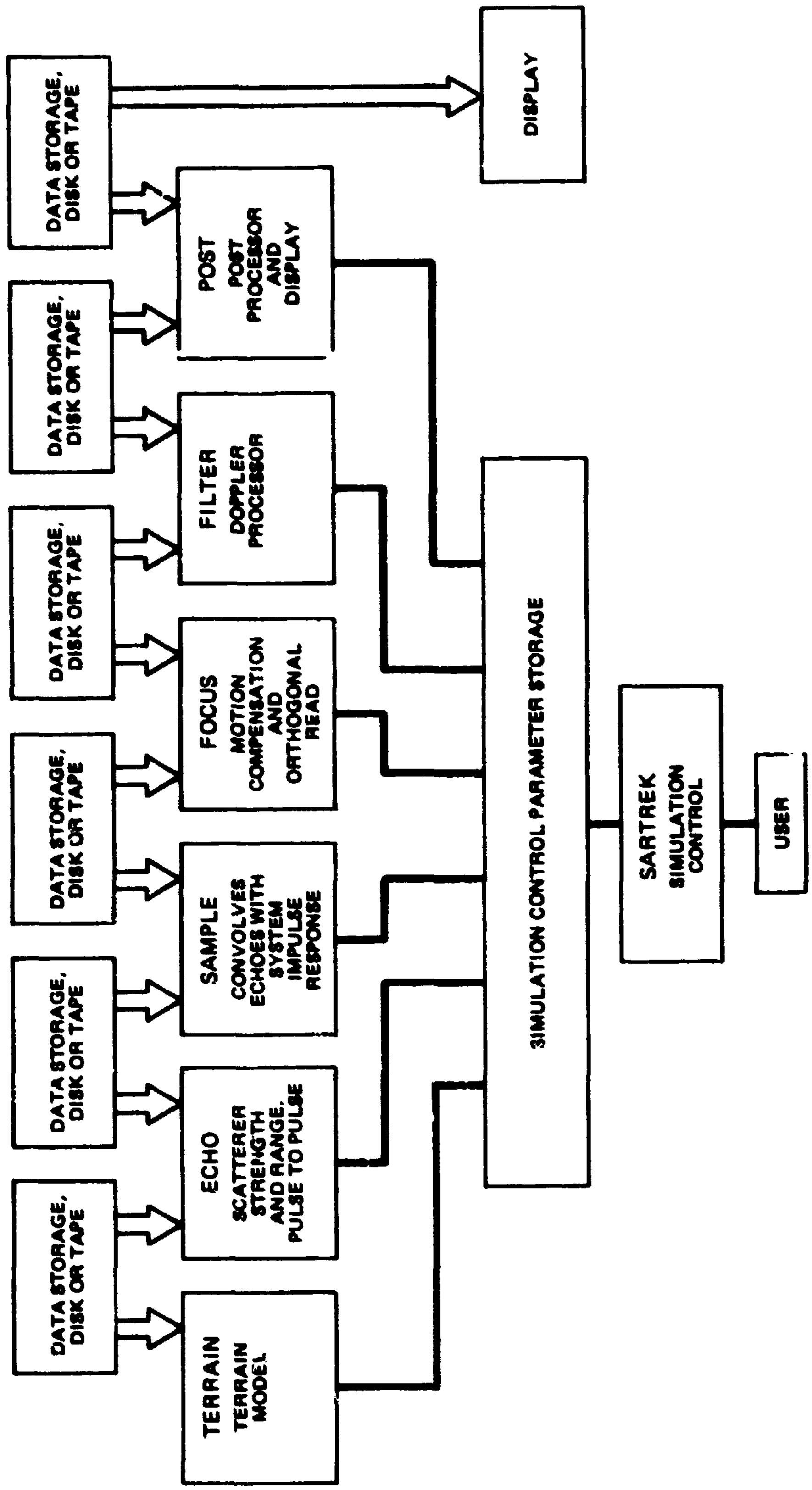

FIGURE 1
SIMULA' ION ARCHITECTURE

ARL:UT
AE-81-130
CRG - GA
9 - 16 - 81

ORIGINAL PAGE
BLACK AND WHITE PHOTOGRAPH

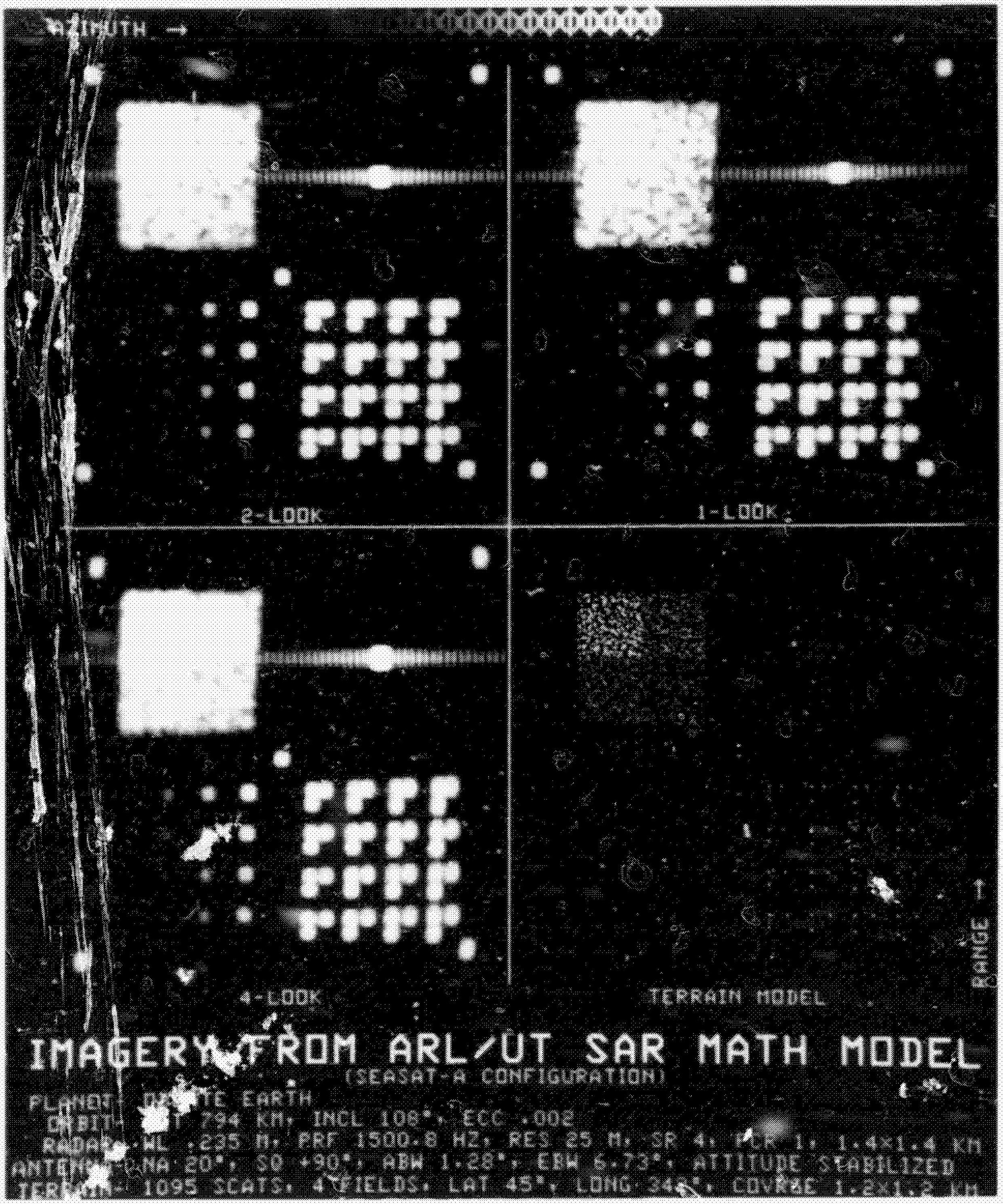

FIGURE 2
IMAGERY FROM ARL:UT SYNTHETIC APERTURE RADAR (SAR) MATH MODEL

3931

These are normalized Stokes parameters, defined as follows, with reference to Fig. 3:

$$Ex = E_o \cos\varepsilon \sin\omega t \cos\tau - E_o \sin\varepsilon \cos\omega t \sin\tau \tag{17}$$

$$Ey = E_o \cos\varepsilon \sin\omega t \sin\tau + E_o \sin\varepsilon \cos\omega t \cos\tau \quad . \tag{18}$$

If we now substitute the time dependent values of Ex and Ey we have

$$E_1 \sin(\omega t-\delta_1) = E_o(\cos\varepsilon \sin\omega t \cos\tau - \sin\varepsilon \cos\omega t \sin\tau) \tag{19}$$

$$E_2 \sin(\omega t-\delta_2) = E_o(\cos\varepsilon \sin\omega t \sin\tau + \sin\varepsilon \cos\omega t \cos\tau) \quad . \tag{20}$$

If these are expanded, and $\sin\omega t$ terms and $\cos\omega t$ terms set equal (which eliminates the time dependence):

$$E_1 = E_o\left(\cos^2\varepsilon \cos^2\tau + \sin^2\varepsilon \sin^2\tau\right)^{1/2} \tag{21}$$

$$E_2 = E_o\left(\cos^2\varepsilon \sin^2\tau + \sin^2\varepsilon \cos^2\tau\right)^{1/2} \quad . \tag{22}$$

The flux density in W/m^2 is the Poynting vector $\bar{S}$:

$$|\bar{S}| = S_x + S_y = \frac{E_1^2 + E_2^2}{Z_o} = \frac{E_o^2}{Z_o} \quad , \tag{23}$$

where Z_o is the free space impedance, 377 Ω per square measure, S_x is the Poynting vector for the E_o wave component polarized to x, and S_y, for the one polarized to y.

$$S_x = \frac{E_1^2}{Z_o} = |\bar{S}|(\cos^2\varepsilon \cos^2\tau + \sin^2\varepsilon \sin^2\tau) \tag{24}$$

$$S_y = \frac{E_2^2}{Z_o} = |\bar{S}|(\cos^2\varepsilon \sin^2\tau + \sin^2\varepsilon \cos^2\tau) \quad .$$

The Stokes parameters are now defined as

$$s_o = \frac{S}{S} = 1$$

$$s_1 = \frac{S_x - S_y}{S} = \frac{\left\langle E_1^2\right\rangle - \left\langle E_2^2\right\rangle}{SZ} = \cos 2\varepsilon \cos 2\tau \quad , \tag{25}$$

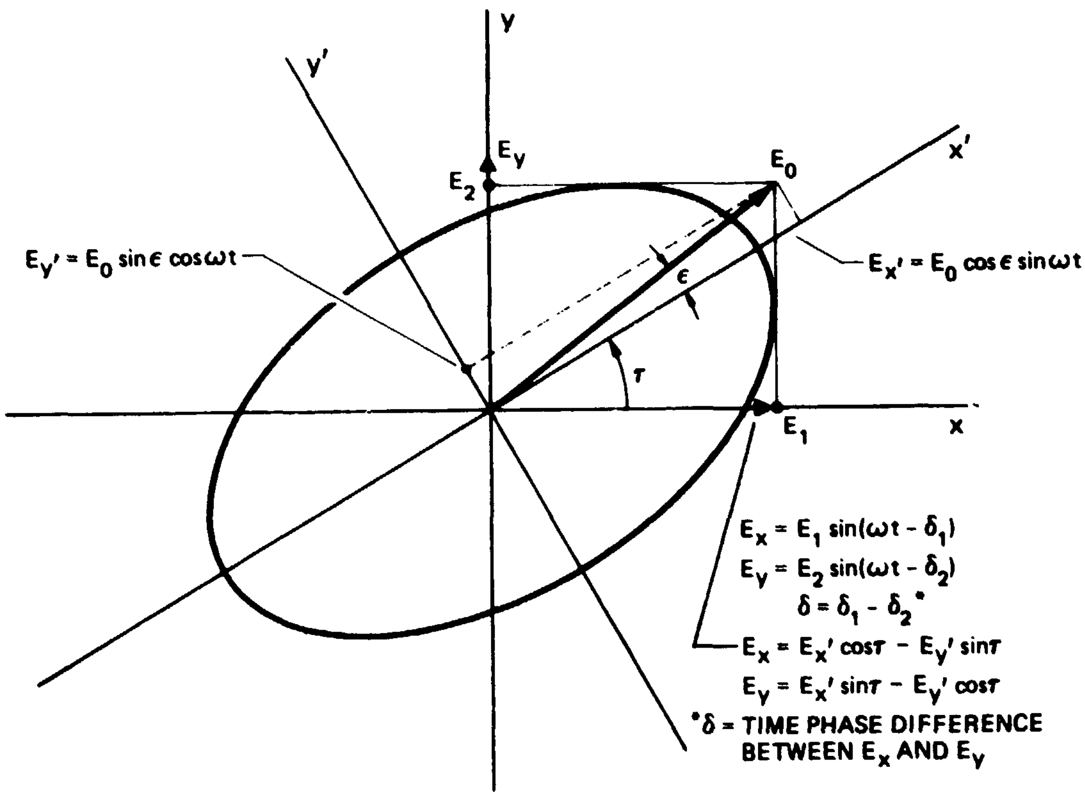

FIGURE 3
POLARIZATION ELLIPSE

ARL:UT
AE-81-131
CRG - GA
9 - 16 - 81

where <> denotes time averaged value. Then

$$s_2 = \frac{2}{SZ} <E_1 \; E_2 \cos\delta> = <\cos 2\varepsilon \; \sin 2\tau> \quad ,$$

$$s_3 = \frac{2}{SZ} <E_1 \; E_2 \cos\delta> = <\sin 2\varepsilon> \quad ,$$

$$1 \geq s_1^2 + s_2^2 + s_3^2 \quad .$$

These can be written in matrix form

$$S[s_i] = S\begin{bmatrix} s_o \\ s_1 \\ s_2 \\ s_3 \end{bmatrix} \quad i = 0,1,2,3 \tag{26}$$

$$= S\begin{bmatrix} 1-d \\ 0 \\ 0 \\ 0 \end{bmatrix} + S\begin{bmatrix} d \\ d \cos 2\varepsilon \cos 2\tau \\ d \cos 2\varepsilon \sin 2\tau \\ d \sin 2\varepsilon \end{bmatrix} \tag{27}$$

for a partially polarized wave, where the first term of Eq. (27) is the polarized power density and the second is the unpolarized power density.

The antenna polarization response may also be expressed as a matrix, with A_e the effective aperture:

$$A_e[a_i] = A_e\begin{bmatrix} a_o \\ a_1 \\ a_2 \\ a_3 \end{bmatrix} m^2 \tag{28}$$

Thus the power out of the antenna is given by

$$W = \frac{1}{2} S \; A_e[a_i]_t \; [s_i]$$

$$= \frac{1}{2} S \; A_e \sum_{i=o}^{3} a_i \; s_i \quad W/Hz \tag{29}$$

The simulation for the APQ-102 uses a linear polarized antenna, with a gain given by

$$G = \frac{4\pi A_e}{\lambda^2} \quad , \tag{30}$$

and the magnitude of the gain function can be entered into the simulation via program ANTENA. Substituting the matrix representation for the A_e we have

$$G[a_i] = \frac{4\pi}{\lambda^2} A_e[a_i] = \frac{4\pi}{\lambda} A_e \begin{bmatrix} a_o \\ a_1 \\ a_2 \\ a_3 \end{bmatrix} \tag{31}$$

Combining the polarization matrix for a scatterer, we have

$$G[a_i, s_i] = \frac{4\pi}{\lambda^2} \frac{|\sigma|}{2} [a_o a_1 a_2 a_3] \begin{bmatrix} s_o \\ s_1 \\ s_2 \\ s_3 \end{bmatrix} \tag{32}$$

where the substitution of radar cross-section σ is made for the power density S, assuming that the backscattered power density is proportional to the cross section.

To implement this function in program ANTENA requires that the a_i be specified, as well as the s_i. The former may reduce to $a_o=1$, $a_1=0$, $a_2=0$, $a_3=0$, or it may depend on platform motion.

The specification of [s] on the other hand would be arbitrary or would depend on measured data for particular types of radar targets or clutter.

As a first step, it was decided to investigate the effects of crosspolarized antennas for transmit and receive, and assume no polarization sensitivity for σ. Although the crosspolarized response of the receive antenna has been measured, it was not available in the azimuth plane, only in elevation. Based on the lobe structure and boresight gain of the elevation pattern, a crosspolarized azimuth response pattern was constructed and used to specify ANTENA. Figure 4 illustrates the pattern used.

The values for the patterns, digitized every 0.33° to a coverage of ±24°, were entered using an HP9810A with digitizer. The SEASAT radar parameters were used and six scatterers were entered into the terrain model for test purposes. Five of these were given a cross section of 1 m^2 at the center and corners of the 1.4 x 1.4 km mapped area; the other was 26 dB greater at 20 m^2. The simulation was exercised and the SARCON data were printed out--see the Appendix. Figure 5 shows the displayed results for the co-polarized antenna response. Post-processing was effected at 2 dB/gray shade, with the peak filter magnitude falling in gray shade 16. Figure 5(a) has gray shade 16 turned on and Fig. 5(b) has it off. To expedite processing no range pulse compression was used; hence range sidelobes are not present. Figure 6 is for the same scatterer array but uses a unit antenna pattern, i.e., it is isotropic. There is no appreciable difference since the entire imaged area falls well within the beam of the APQ-102 1.3° 3 dB beamwidth for the orbiter altitude of 870 km.

To demonstrate antenna response, a realistic terrain scene without a prohibitively large scattering area was required and it was necessary to place scatterers at ambiguous (with respect to pulse repetition frequency (PRF)) response points. The total azimuth coverage imaged was only 1.4 km; if the terrain model covered only this area, then from an altitude of 870 km along 4.6 km of the orbit (the synthetic array length), only ±0.25° of the antenna patterns would be used. To create an effective but simple model of terrain, single scatterers were placed at ambiguous points as illustrated in Fig. 7. Only the single scatterer

ORIGINAL PAGE
BLACK AND WHITE PHOTOGRAPH

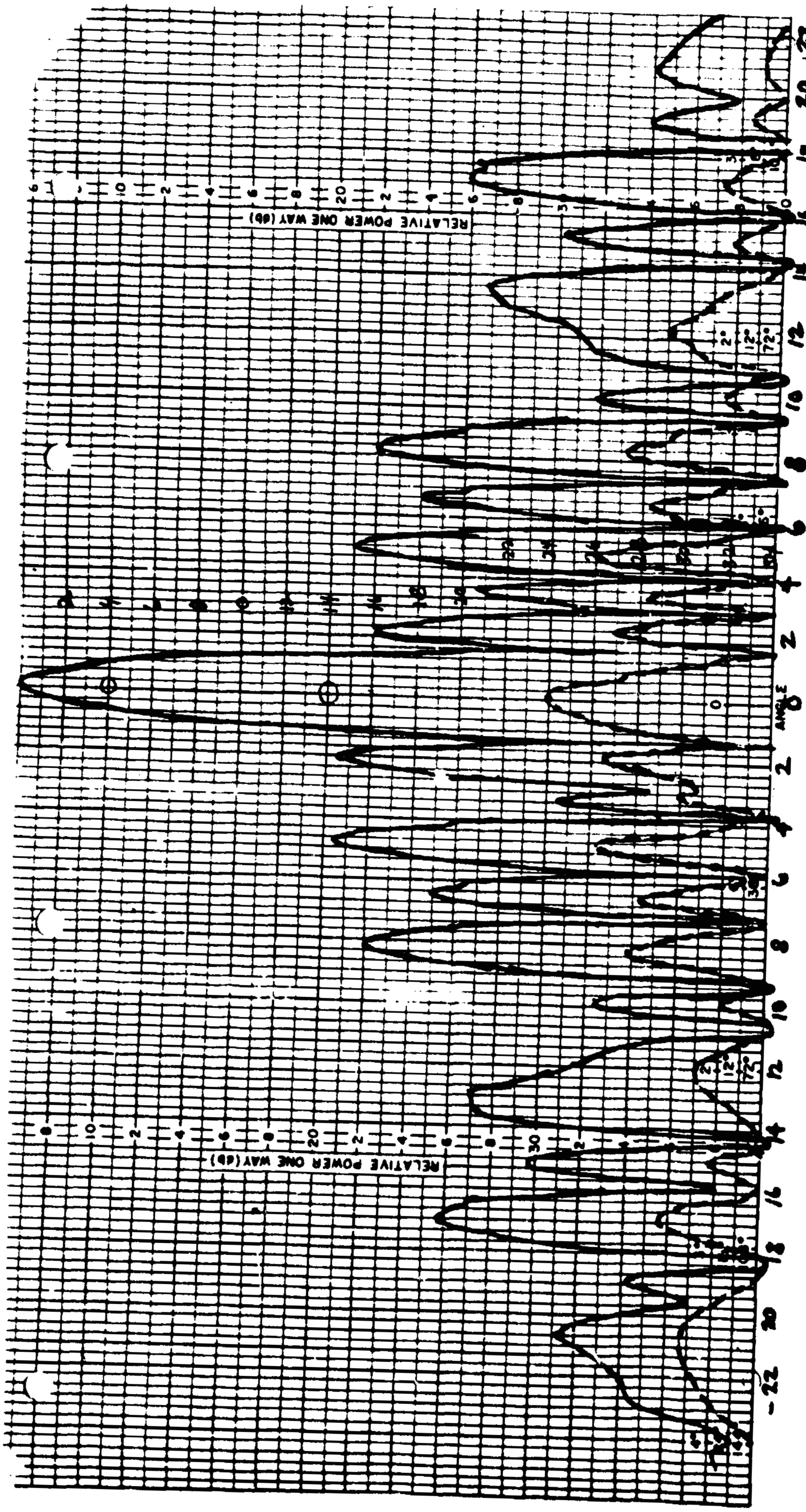

AN/APQ-102
40° ELEVATION

—— CO-POLARIZED ANTENNA RESPONSE

------ CROSSPOLARIZED ANTENNA RESPONSE

FIGURE 4
APQ-102 ANTENNA SIMULATION PATTERNS

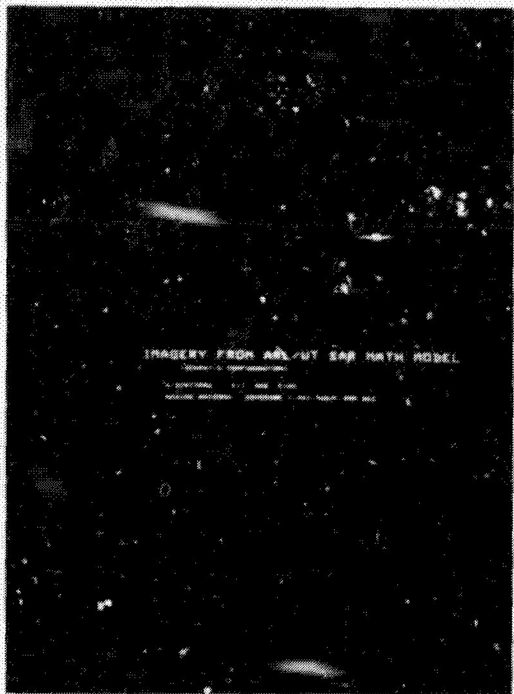

(a) Six-scatter OSS simulation, all gray shades, brightness on display set for minimum Doppler sidelobes on 100 x scatterer

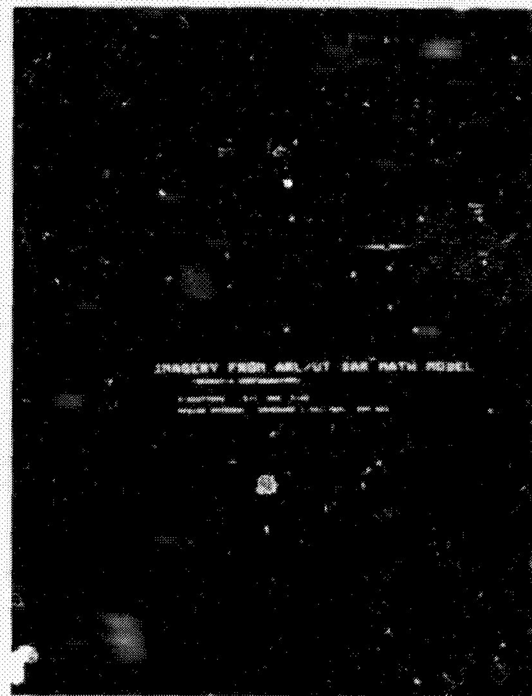

(b) Gray shade 16 turned off, brightness increased to include all Doppler filter sidelobes

FIGURE 5

OSS SIMULATION OF SIX-SCATTERER ARRAY USING SEASAT SYSTEM
WITH APQ-102 ANTENNA PATTERN IN AZIMUTH,
NO PULSE COMPRESSION

AE-81-133

ORIGINAL PAGE
BLACK AND WHITE PHOTOGRAPH

(a) Six-scatter OSS simulation, all gray shades, brightness on display set for minimum Doppler sidelobes on 100 x scatterer

(b) Gray shade 16 turned off, brightness increased to include all Doppler filter sidelobes

FIGURE 6
OSS SIMULATION OF SIX-SCATTERER ARRAY USING SEASAT SYSTEM
WITH UNIT ANTENNA PATTERN IN AZIMUTH,
NO PULSE COMPRESSION

AE-81-134

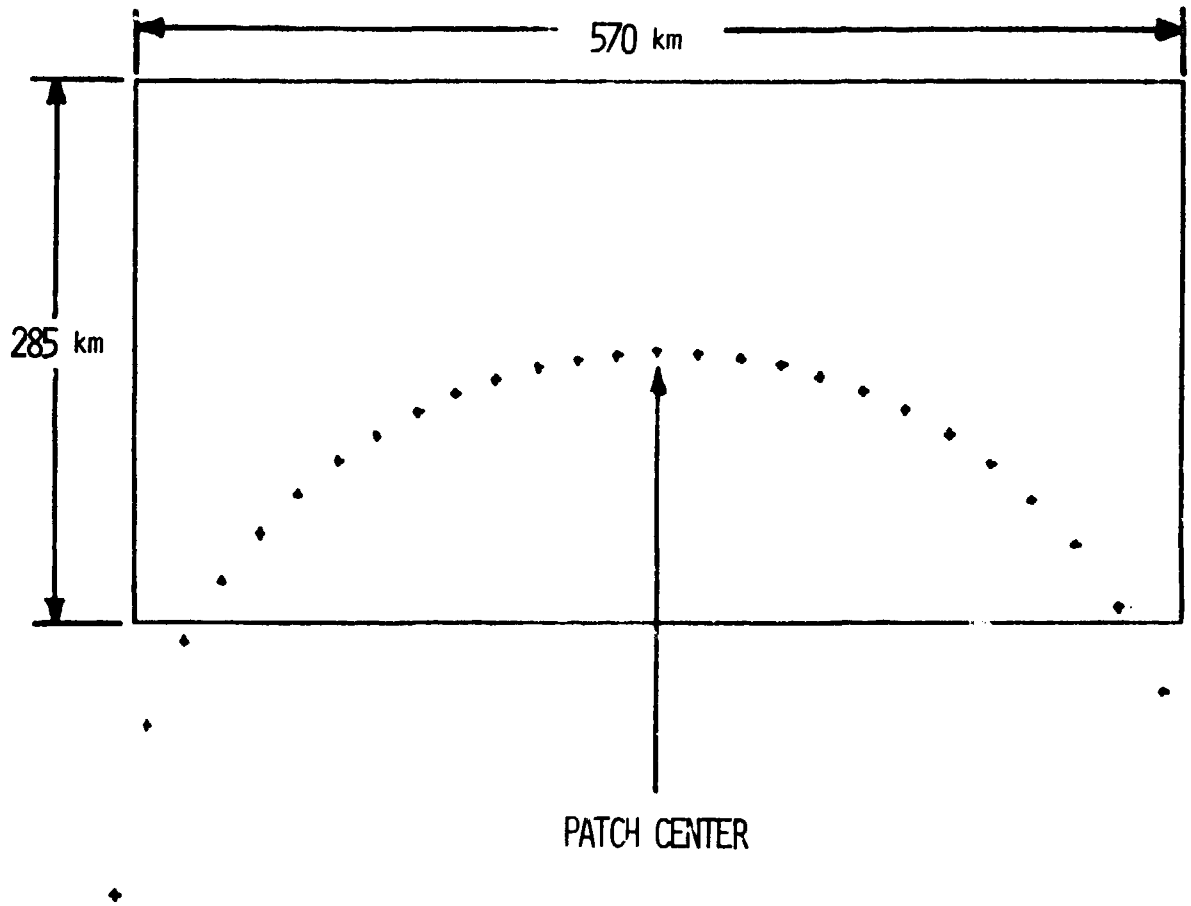

27 Discrete Scatterers in Model

FIGURE 7
AMBIGUITY TERRAIN

at the patch center was imaged; however, there were Doppler contributions from all the sidelobe scatterers. Two configurations of scatterers were used; the second one offset the ambiguous point scatterers in graduated steps 10-30 m from the ambiguity locations.

Figure 8 illustrates the results. Each photograph contains six images of the patch center; each of these is 1.4 x 0.4 km, with 25 m resolution. From the top, the first three strips are of the unoffset terrain model imaged with the isotropic, co-polarized, and crosspolarized patterns. All three patterns were normalized to 1.0 at the peak response. The last three from the top on the left are images of the offset scatterers for co-polarized, crosspolarized, and isotropic patterns. The top gray shade of the display is set down 20 dB from the peak response of the center pixel to show the weak sidelobe structure.

The right photo has the same order of images, but the top gray shade is 35 dB below the peak response, thus defining more clearly sidelobe response of the system configurations.

Analysis of these results shows a significant reduction in ambiguities between images with the isotropic antenna pattern and the APQ-102 patterns. The co-polarized pattern image shows no ambiguities and has lower sidelobes than the crosspolarized image. The cross-polarized pattern generates an ambiguity due to its high sidelobes. One must be careful in trying to interpret the power level of the ambiguities, because the energy returned outside the main beam is from only a few scatterers and may be lower than the energy returned from an actual continuous terrain area.

B. Frequency Diversity Effects

It was decided to investigate the image variations with wavelength on the scene of Fig. 2, which has been imaged at the SEASAT wavelength of 23.5 cm. Three other wavelengths were selected: 1.8, 3.125, and 10.34 cm.

ORIGINAL PAGE
BLACK AND WHITE PHOTOGRAPH

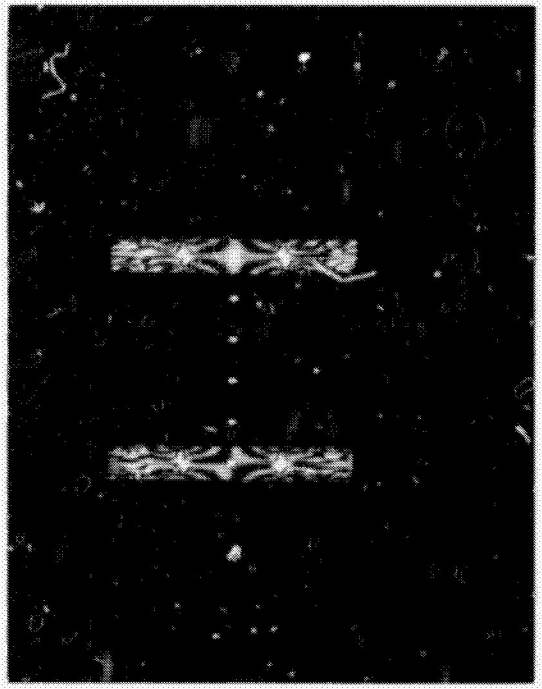

(a) Top gray shade of display set 20 dB down from the imaged pixel at the patch center

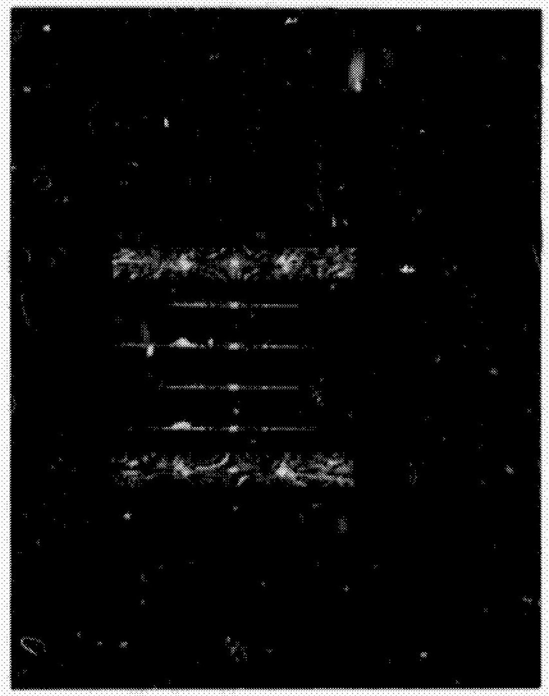

(b) Top gray shade of display set 35 dB from the imaged pixel at the patch center

FIGURE 8

RESULTS FROM SAR SIMULATION PROGRAM

To properly implement the simulation the variation of the cross section with wavelength should be included. Other wavelength dependent factors are the antenna response patterns, transmitted power, receiving system noise and, indeed, every factor in the radar range equation either implicitly or directly. In the interest of economy and reduced complexity, however, only the effects on the synthetic array processing were taken into account. The results are not very dramatic, as would be the case if, for example, the cross-section dependency were included. This could involve a simple adjustment since, generally speaking, radar cross section varies proportionally to the square of the wavelength. A useful set of relations might be:

$$\sigma_L = 1\ \mathrm{m}^2 \qquad = 0\ \mathrm{dB\ m}^2$$

$$\sigma_S = \frac{\sigma_L (10.34)^2}{(23.5)^2} = 1.936 \times 10^{-1}\ \sigma_L = -7\ \mathrm{dB\ m}^2$$

$$\sigma_X = \frac{\sigma_L (3.125)^2}{(23.5)^2} = 1.768 \times 10^{-2}\ \sigma_L = -17.5\ \mathrm{dB\ m}^2$$

$$\sigma_{Ku} = \frac{\sigma_L (1.8)^2}{(23.5)^2} = 5.867 \times 10^{-3}\ \sigma_L = -24\ \mathrm{dB\ m}^2$$

This is in general true only for perfectly conducting bodies, and is not the general case for clutter targets. For the first simulation effort, only the wavelength parameter was varied, and the resolution cell dimensions were forced to the same values by varying the number of pulses processed or, equivalently, the array length.

Figure 9 presents the four images of the test pattern, photographed with two different exposures. The most obvious effect of the wavelength changes is in the coherent speckle pattern for the homogeneous fields. The data were analyzed statistically, and only very slight changes in the average values were observed. Table IV provides these data for comparison. The simulations were run for the SEASAT radar and the isotropic antenna pattern. The ARL:UT high resolution display system was used to display and photograph the results (Fig. 10).

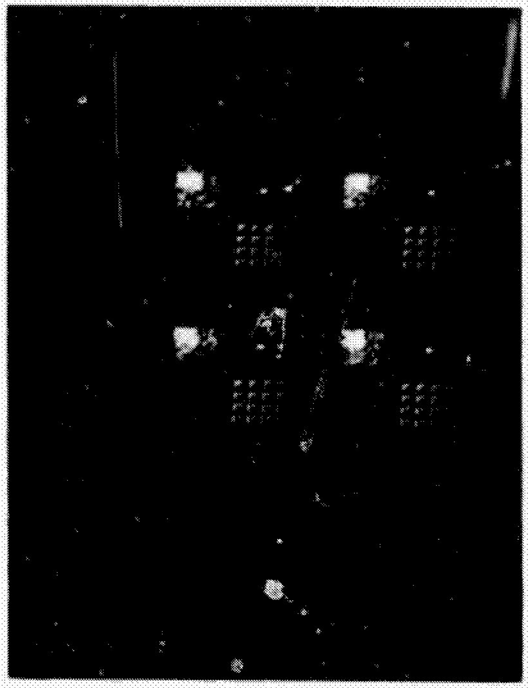

Range ↑

Azimuth →

1-B f8, 1/4 sec exposure
ASA 3000

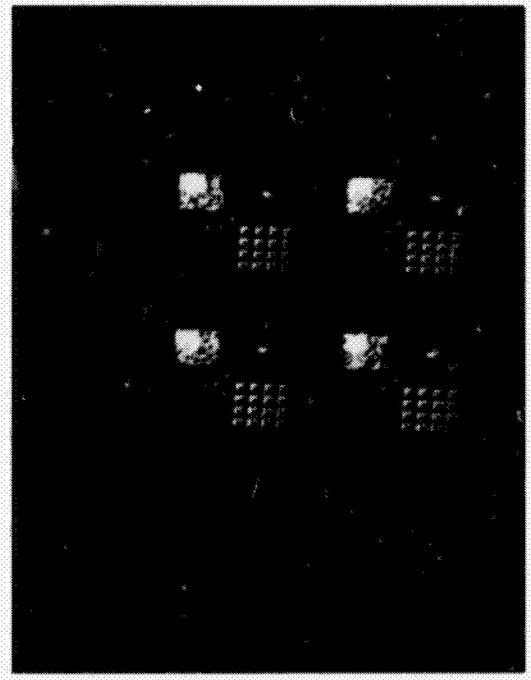

Range ↑

Azimuth →

1-A f8, 1/2 sec exposure
ASA 3000

FIGURE 9

TEST SCENE, WAVELENGTH DIVERSITY

Clockwise From Lower left: L, S, X, K_u Band

TABLE IV

PARTIAL RESULTS OF FREQUENCY DIVERSITY STUDY

STATISTICAL DATA

	Wavelength			
Filter Magnitude	23.5 (cm)	10.345 (cm)	3.125 (cm)	1.8 (cm)
Maximum	336.63147	337.97644	334.47785	342.83377
Minimum	6.86×10^{-12}	3.69×10^{-14}	5.13×10^{-13}	8.95×10^{-15}
Mean	0.18181	0.17562	0.17848	0.180995
Sigma	4.857	4.859	4.849	4.959

SYNTHETIC ARRAY PARAMETERS

Array No. 1	43,262 pts	43,039 pts	42,816 pts	42,816 pts
Array Length, m	4602	2026	612	352.5
Formation Time (sec)	0.617	0.271	0.082	0.047
No. of Pulses	926	916	900	896
PRF, Hz	1,500	3,370	10,970	18,948
Platform Velocity (km/sec)	7.4577	7.4577	7.4577	7.4577

The PRF was increased to obtain approximately the same number of samples (pulses) in array lengths progressively shorter so that resolution would remain the same for the azimuth dimension as wavelength decreased. Had this not been done, the azimuth resolution would have drastically increased as the ratio of array length to wavelength increased.

ORIGINAL PAGE
BLACK AND WHITE PHOTOGRAPH

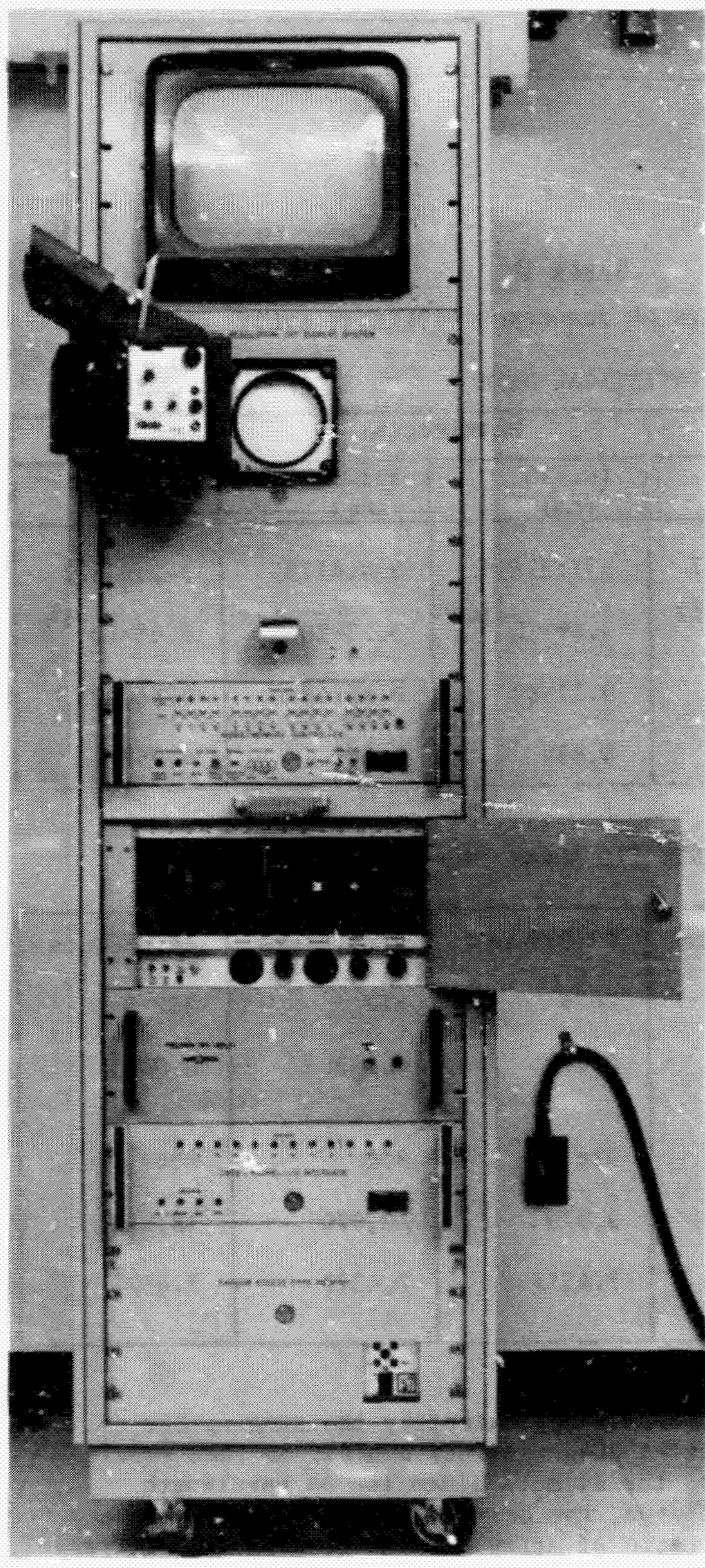

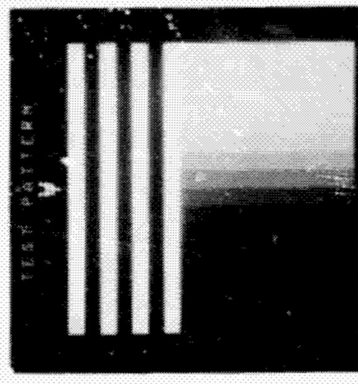

CALIBRATION PATTERN

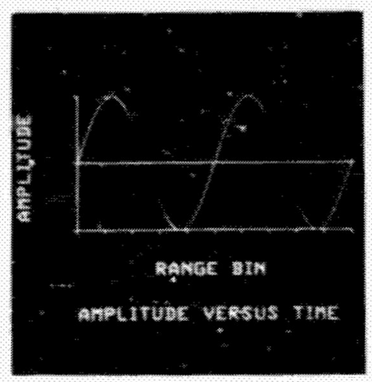

GRAPHICS

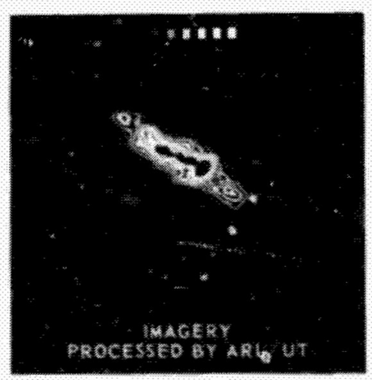

IMAGE CONTOURS FROM
SELECTED GREY SHADES

FIGURE 10
ARL:UT HIGH RESOLUTION DISPLAY SYSTEM

2838-14A

IV. TECHNICAL EFFORT SUMMARY

Unfortunately, the dilution of the resources allocated to the simulation efforts by the ASAR project prevented completion of in-depth studies on any of the subjects undertaken. Initial analysis was commenced on a wide swath technique using squinted multiple beams. A major challenge will be the formation of the image from the output of multiple beams tracking the clutter along the velocity vector. Figure 11 illustrates the concept, which will be undertaken in a follow-on effort.

In summary, the ASAR work provided a method for adapting the OSS simulation to an aircraft platform, and to a linear FM (chirped) pulse radar. The analysis indicates the approach to be taken to fully characterize the effects of polarization of the backscattered energy and crosspolarization of the antenna system versus co-polarization of transmit and receive antennas.

Finally, some effects of frequency diversity in the generation of coherent speckle from homogeneous fields were synthesized with the simulation. These efforts point the way to more detailed and fruitful investigations in the future, using the OSS simulation programs.

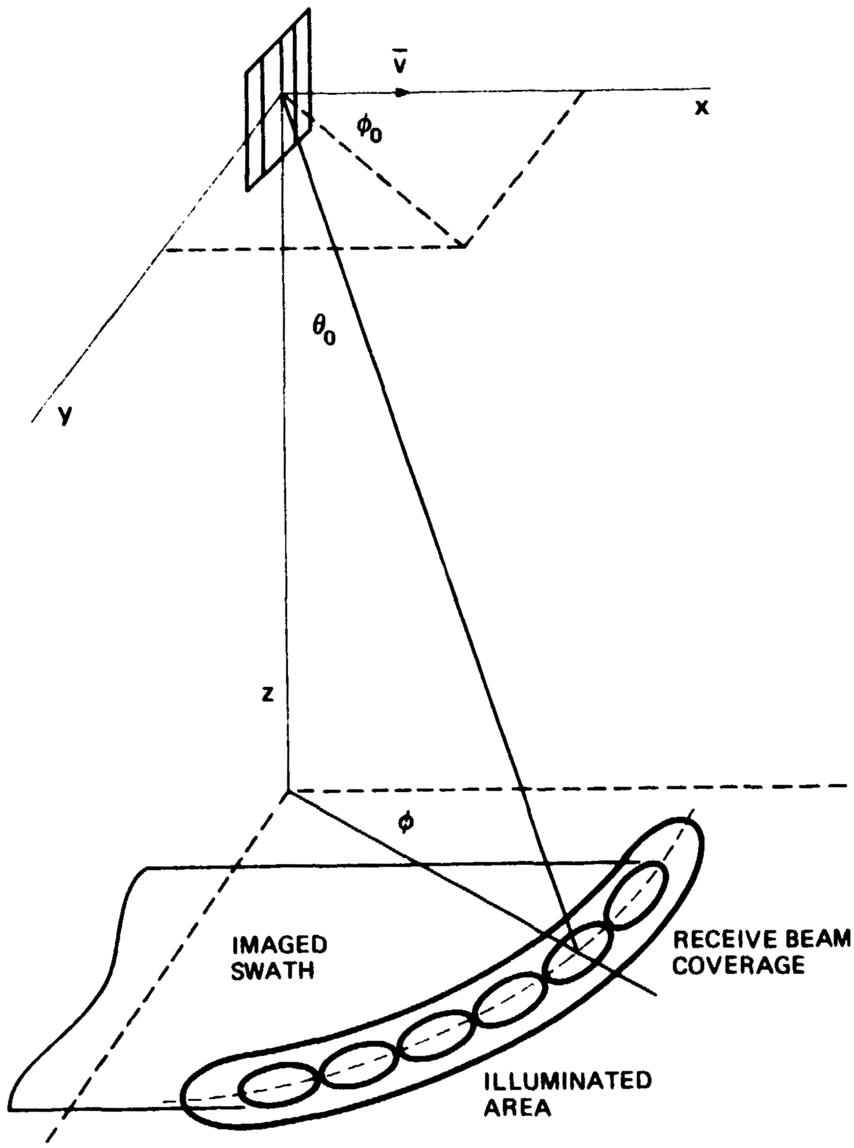

FIGURE 11
THE GEOMETRY OF THE MULTIPLE BEAM SAR

ARL:UT
AE-81-137
CRG - GA
9 - 16 - 81

L-BAND WAVELENGTH DATA

PRECEDING PAGE BLANK NOT FILMED

```
--------- PROGRAM FILTER IN EXECUTION ----------
INPUT KBRANCH
INPUT IFILTOF,IFILIMG                          0
NPUT I/O DATA ON IODATF     , FILE 1
UTPUT IMAGE DATA ON CIMAGE     , FILE 8
FT SAMPLE INTERVAL IS SET AT SIA/1
O. OF FILTERS REQUIRED FOR FULL PRF COVERAGE IS 3 .6
RESUM RATIO OF 14 IS DERIVED FROM A SAMPLE POINT ERROR TOLERANCE OF .002
O. OF PRESUMMED FFT FILTERS IS 230
```

```
* * * * * * * * *   P L A N E T   S P E C I F I C A T I O N   * * * * * * * * *
PLANET NAME  **                       EARTH              EQUATORIAL RADIUS (KM)  **                    .63781670000E+04
ECCENTRICITY  **                      .81820179996E-01 GRAVITATIONAL CONSTANT (KM3/SEC2)  ** .39860100000E+06
ROTATIONAL RATE (DEG/S)  **           .41780745995E-02 TIME OF PRIME MERIDIAN PASSAGE (S) **0.

* * * * * * * * *   O R B I T   S P E C I F I C A T I O N   * * * * * * * * *
ORBIT I.D.  **                        794CIRCUL          SEMI-MAJOR AXIS (KM)  **                     .71865400000E+04
ECCENTRICITY  **                      .20000000000E-02 INCLINATION (DEG)  **                          .10800000000E+03
LONG OF ASCENDING NODE (DEG)  **    0.                   ARGUMENT OF PERIGEE (DEG)  **              0.
TIME OF PERIGEE PASSAGE (S)  **     0.                   ROTATIONAL RATE (DEG/S)  **                .59376152657E-01
ORBITER INITIALIZATION TIME(S)  **  -.10000000000E-03

* * * * * * * * *   R A D A R   S P E C I F I C A T I O N   * * * * * * * * *
RADAR I.D.  **                        SEASAT-A           OPERATING WAVELENGTH (M)  **                .23500000000E+00
RECIEVER/TRANSMITTER BW (MHZ)  **     .15549599534E+02 RANGE TIME-BANDWIDTH PRODUCT  **              .10000000000E+01
SIGNAL-TO-NOISE RATIO (DB)  **        .10000000000E+03 A/D SAMPLE RATE (MHZ)  **                     .62198398135E+02
SAMPLE LENGTH OF RANGE CORRELATION **                1 SAMPLE LENGTH ACROSS PHASE INTERVAL *                      1
BINARY PHASE CODE  **                 R                  BINARY PHASE CODE SEQUENCE  **              RANDOM
GROUND RANGE RESOLUTION (M)  **       .25000000000E+02 AZIMUTH RESOLUTION (M)  **                    .25000000000E+02
RANGE SAMPLING RATIO (M)  **          .40000000000E+01 AZIMUTH SAMPLING RATIO (M)  **                .40000000000E+01
RANGE IMPULSE RESPONSE FUNCTION  **   COSINE**2          APERTURE WEIGHT FUNCTION  **                TAYLOR
PATCH-TO-PATCH OFFSET, RNG (M)  **  0.                   PATCH-TO-PATCH OFFSET, AZ (M)  **          0.
RANGE SWATH WIDTH (KM)  **            .14000000000E+01 NO OF PATCHES  **                                          1
MAP START LATITUDE (DEG)  **          .45000000000E+02

* * * * * * * * *   A N T E N N A   S P E C I F I C A T I O N   * * * * * * * * *
ANTENNA I.D.  **                      UNITPAT            BORESIGHT NADIR AT TO (DEG)  **             .20000000000E+02
BORESIGHT SQUINT AT TO (DEG)  **      .90000000000E+02 AZIMUTH ANGULAR COVERAGE (DEG)  **            .12800000000E+01
ELEVATION ANGULAR COVERAGE (DEG)  **  .67300000000E+01 PHASE CENTER, BODY AXIS X (M)  **           0.
PHASE CENTER, BODY AXIS Y (M)  **   0.                   PHASE CENTER, BODY AXIS Z (M)  **          0.
COORD SYS, BODY AXIS ROLL, (DEG)  ** 0.                  COORD SYS, BODY AXIS PITCH, (DEG) ** -.70000000000E+02
COORD SYS, BODY AXIS YAW, (DEG)  **   .90000000000E+02 PLAT ROLL RATE (DEG/S)  **                 0.
PLAT PITCH RATE (DEG/S)  **         0.                   PLAT YAW RATE (DEG/S)  **                  0.

* * * * * * * * *   T E R R A I N   S P E C I F I C A T I O N   * * * * * * * * *
TERRAIN I.D.  **                      TESTPATERN         NO OF DISCRETES  **                                     71
NO OF FIELDS  **                                     4 TOTAL NO OF SCATTERERS  **                              1095
X-AXIS COVERAGE (KM)  **              .12000000000E+01 Y-AXIS COVERAGE (KM)  **                      .12000000000E+01
TERRAIN CENTER, R (KM)  **            .63675192370E+04 TERRAIN CENTER, LAT (DEG)  **                 .45000000000E+02
TERRAIN CENTER, LONG (DEG)  **        .34191125864E+03
```

```
****** S Y N T H E T I C   A R R A Y   P A R A M E T E R S ******
SYNTHETIC ARRAY NO  **                                   1 TRANSMISSION START TIME (S)  **          .78561515863E+03
ARRAY LENGTH (M)  **                      .46023487081E+04 ARRAY INCLINATION (DEG)  **              .83463340843E-01
ARRAY FORMATION TIME (MS)  **             .61712748885E+03 PLATFORM VELOCITY (KM/S)  **             .74576917166E+01
NO OF PULSES  **                                       926 PRF (HZ)  **                             .15003017230E+04
NO OF RANGE SAMPLES  **                                223 NO. OF AZIMUTH FILTERS  **                            223
PATCH CENTER RANGE SAMPLE NO.  **                      112 SLANT RANGE SWATH WIDTH (KM)  **         .53983302281E+00
SLANT RANGE RESOLUTION (M)  **            .96398784853E+01 SLANT RANGE SAMPLE INTERVAL (M)  **      .24099696213E+01
START RANGE (KM)  **                      .86825086019E+03 RANGE PATCH CENTER (KM)  **              .86851836682E+03
SQUINT ANGLE PATCH CENTER (DEG)  **       .90400904630E+02 NADIR ANGLE PATCH CENTER (DEG)  **       .20006044097E+02
LOS AZIMUTH AT PATCH CENTER (DEG) **     -.11260159984E+03 LOS INCIDENCE AT PATCH CENTER (DEG)**    .22680692212E+02
PATCH CENTER, R (KM)  **                  .63675192370E+04 ORBITER MASS CENTER, R (KM)  **          .71766915525E+04
PATCH CENTER, LAT (DEG)  **               .45000000000E+02 ORBITER MASS CENTER, LAT (DEG)  **       .43920144547E+02
PATCH CENTER, LONG (DEG)  **              .34191125864E+03 ORBITER MASS CENTER, LONG (DEG)  **      .33848242890E+03
PATCH CENTER PIXEL POWER IS .9999974269902

        ARRAY STATISTICS FOR  43262 POINTS.
MAXIMUM 336.6314724528,  MINIMUM 6.861199744928E-12
MEAN .1818136300036,  SIGMA 4.857006193401
EOF WRITTEN ON CIMAGE    , AFTER RECORD 224
```

S-BAND WAVELENGTH DATA

PRECEDING PAGE BLANK NOT FILMED

```
--------- PROGRAM FILTER IN EXECUTION ----------
INPUT KBRANCH
INPUT IFILIOF,IFILIMG
NPUT I/Q DATA ON IQDATF     , FILE 1
UTPUT IMAGE DATA ON CIMAGE     , FILE 7
FT SAMPLE INTERVAL IS SET AT SIA/1
O. OF FILTERS REQUIRED FOR FULL PRF COVERAGE IS 3180
RESUM RATIO OF 14 IS DERIVED FROM A SAMPLE POINT ERROR TOLERANCE OF .002
O. OF PRESUMMED FFT FILTERS IS 227
```

```
* * * * * * * * * *   P L A N E T   S P E C I F I C A T I O N   * * * * * * * * * *
PLANET NAME  **                              EARTH             EQUATORIAL RADIUS (KM)  **                     .63781670000E+04
ECCENTRICITY  **                             .81820179996E-01  GRAVITATIONAL CONSTANT (KM3/SEC2)  **          .39860100000E+06
ROTATIONAL RATE (DEG/S)  **                  .41780745995E-02  TIME OF PRIME MERIDIAN PASSAGE (S)  **         0.

* * * * * * * * * *   O R B I T   S P E C I F I C A T I O N   * * * * * * * * * *
ORBIT I.D.  **                               794CIRCULR        SEMI-MAJOR AXIS (KM)  **                       .71865400000E+04
ECCENTRICITY  **                             .20000000000E-02  INCLINATION (DEG)  **                          .10800000000E+03
LONG OF ASCENDING NODE (DEG)  **             0.                ARGUMENT OF PERIGEE (DEG)  **                  0.
TIME OF PERIGEE PASSAGE (S  **               0.                ROTATIONAL RATE (DEG/S)  **                    .59376152657E-01
ORBITER INITIALIZATION TIME(S)  **           -.10000000000E-03

* * * * * * * * * *   R A D A R   S P E C I F I C A T I O N   * * * * * * * * * *
RADAR I.D.  **                               SEASAT-A          OPERATING WAVELENGTH (M)  **                   .10345000000E+00
RECIEVER/TRANSMITTER BW (MHZ)  **            .15552207400E+02  RANGE TIME-BANDWIDTH PRODUCT  **               .10000000000E+01
SIGNAL-TO-NOISE RATIO (DB)  **               .10000000000E+03  A/D SAMPLE RATE (MHZ)  **                      .62208?9602E+02
SAMPLE LENGTH OF RANGE CORRELATION  **                      1  SAMPLE LENGTH ACROSS PHASE INTERVAL  *                        1
BINARY PHASE CODE  **                        R                 BINARY PHASE CODE SEQUENCE  **                 RANDOM
GROUND RANGE RESOLUTION (M)  **              .25000000000E+02  AZIMUTH RESOLUTION (M)  **                     .25000000000E+02
RANGE SAMPLING RATIO (M)  **                 .40000000000E+01  AZIMUTH SAMPLING RATIO (M)  **                 .40000000000E+01
RANGE IMPULSE RESPONSE FUNCTION  **          COSINE**2         APERTURE WEIGHT FUNCTION  **                   TAYLOR
PATCH-TO-PATCH OFFSET, RNG (M)  **           0.                PATCH-TO-PATCH OFFSET, AZ (M)  **              0.
RANGE SWATH WIDTH (KM)  **                   .14000000000E+01  NO OF PATCHES  **                                             1
MAP START LATITUDE (DEG)  **                 .45000000000E+02

* * * * * * * * *   A N T E N N A   S P E C I F I C A T I O N   * * * * * * * * *
ANTENNA I.D.  **                             UNITPAT           BORESIGHT NADIR AT TO (DEG)  **                .20000000000E+02
BORESIGHT SQUINT AT TO (DEG)  **             .90000000000E+02  AZIMUTH ANGULAR COVERAGE (DEG)  **             .12800000000E+01
ELEVATION ANGULAR COVERAGE (DEG)  **         .67300000000E+01  PHASE CENTER, BODY AXIS X (M)  **              0.
PHASE CENTER, BODY AXIS Y (M)  **            0.                PHASE CENTER, BODY AXIS Z (M)  **              0.
COORD SYS, BODY AXIS ROLL, (DEG)  **         0.                COORD SYS, BODY AXIS PITCH, (DEG)  **          -.70000000000E+02
COORD SYS, BODY AXIS YAW, (DEG)  **          .90000000000E+02  PLAT ROLL RATE (DEG/S)  **                     0.
PLAT PITCH RATE (DEG/S)  **                  0.                PLAT YAW RATE (DEG/S)  **                      0.

* * * * * * * * *   T E R R A I N   S P E C I F I C A T I O N   * * * * * * * * *
TERRAIN I.D.  **                             TESTPATERN        NO OF DISCRETES  **                                          71
NO OF FIELDS  **                                            4  TOTAL NO OF SCATTERERS  **                                 1095
X-AXIS COVERAGE (KM)  **                     .12000000000E+01  Y-AXIS COVERAGE (KM)  **                       .12000000000E+01
TERRAIN CENTER, R (KM)  **                   .63675192370E+04  TERRAIN CENTER, LAT (DEG)  **                  .45000000000E+02
TERRAIN CENTER, LONG (DEG)  **               .34191125864E+03
```

```
       * * * * * *   S Y N T H E T I C   A R R A Y   P A R A M E T E R S   * * * * * *
SYNTHETIC ARRAY NO  **                                      1 TRANSMISSION START TIME (S)  **            .78561515863E+03
ARRAY LENGTH (M)  **                       .20260126547E+04 ARRAY INCLINATION (DEG)  **                 .83449265311E-01
ARRAY FORMATION TIME (S)  **               .27166739882E+03 PLATFORM VELOCITY (KM/S)  **                .74576936637E+01
NO OF PULSES  **                                    916 PRF (HZ)  **                                   .33707138513E+04
NO OF RANGE SAMPLES  **                             223 NO. OF AZIMUTH FILTERS  **                                223
PATCH CENTER RANGE SAMPLE NO.  **                   112 SLANT RANGE SWATH WIDTH (KM)  **                .53974250109E+00
SLANT RANGE RESOLUTION (M)  **             .96382620255E+01 SLANT RANGE SAMPLE INTERVAL (M)  **         .24095655064E+01
START RANGE (KM)  **                       .86822675113E+03 RANGE PATCH CENTER (KM)  **                 .86849421290E+03
SQUINT ANGLE PATCH CENTER (DEG)  **        .90176516786E+02 NADIR ANGLE PATCH CENTER (DEG)  **          .20002551551E+02
LOS AZIMUTH AT PATCH CENTER (DEG) ** -.11282673345E+03 LOS INCIDENCE AT PATCH CENTER (DEG)**        .22676677119E+02
PATCH CENTER, R (KM)  **                   .63675192370E+04 ORBITER MASS CENTER, R (KM)  **             .71766896761E+04
PATCH CENTER, LAT (DEG)  **                .45000000000E+02 ORBITER MASS CENTER, LAT (DEG)  **          .43910854658E+02
PATCH CENTER, LONG (DEG)  **               .34191125864E+03 ORBITER MASS CENTER, LONG (DEG)  **         .33848927478E+03
PATCH CENTER PIXEL POWER IS .9999995288504

        ARRAY STATISTICS FOR  43039 POINTS.
MAXIMUM 337.9764440181,  MINIMUM 3.690676778656E-14
MEAN .1756182193471,  SIGMA 4.858919965889
 OF WRITTEN ON CIMAGE     , AFTER RECORD 224
```

PRECEDING PAGE BLANK NOT FILMED

X-BAND WAVELENGTH DATA

PRECEDING PAGE BLANK NOT FILMED

```
---------- PROGRAM FILTER IN EXECUTION -----------
INPUT KBRANCH                                   0
INPUT IFILIOF,IFILIMG
NPUT I/O DATA ON IODATF     , FILE 1
UTPUT IMAGE DATA ON CIMAGE     , FILE 9
FT SAMPLE INTERVAL IS SET AT SIA/1
O. OF FILTERS REQUIRED FOR FULL PRF COVERAGE IS 3126
RESUM RATIO OF 14 IS DERIVED FROM A SAMPLE POINT ERROR TOLERANCE OF .002
O. OF PRESUMMED FFT FILTERS IS 223
```

```
          * * * * * * * * *   P L A N E T   S P E C I F I C A T I O N   * * * * * * * * *
PLANET NAME **                            EARTH              EQUATORIAL RADIUS (KM) **                     .63781670000E+04
ECCENTRICITY **                           .81820179996E-01  GRAVITATIONAL CONSTANT (KM3/SEC2) ** .39860100000E+06
ROTATIONAL RATE (DEG/S) **                .41780745995E-02  TIME OF PRIME MERIDIAN PASSAGE (S) **0.

          * * * * * * * * *   O R B I T   S P E C I F I C A T I O N   * * * * * * * * *
ORBIT I.D. **                             794CIRCULR         SEMI-MAJOR AXIS (KM) **                       .71865400000E+04
ECCENTRICITY **                           .20000000000E-02  INCLINATION (DEG) **                          .10800000000E+03
LONG OF ASCENDING NODE (DEG) **       0.                     ARGUMENT OF PERIGEE (DEG) **               0.
TIME OF PERIGEE PASSAGE (S) **        0.                     ROTATIONAL RATE (DEG/S) **                    .59376152657E-01
ORBITER INITIALIZATION TIME(S) **    -.10000000000E-03

          * * * * * * * * *   R A D A R   S P E C I F I C A T I O N   * * * * * * * * *
RADAR I.D. **                             SEASAT-A           OPERATING WAVELENGTH (M) **                   .31250000000E-01
RECIEVER/TRANSMITTER BW (MHZ) **          .15553551119E+02  RANGE TIME-BANDWIDTH PRODUCT **               .10000000000E+01
SIGNAL-TO-NOISE RATIO (DB) **             .10000000000E+03  A/D SAMPLE RATE (MHZ) **                      .62214204476E+02
SAMPLE LENGTH OF RANGE CORRELATION **                     1  SAMPLE LENGTH ACROSS PHASE INTERVAL *                    1
BINARY PHASE CODE **                      B                  BINARY PHASE CODE SEQUENCE **               RANDOM
GROUND RANGE RESOLUTION (M) **            .25000000000E+02  AZIMUTH RESOLUTION (M) **                     .25000000000E+02
RANGE SAMPLING RATIO (M) **               .40000000000E+01  AZIMUTH SAMPLING RATIO (M) **                 .40000000000E+01
RANGE IMPULSE RESPONSE FUNCTION **        COSINE**2          APERTURE WEIGHT FUNCTION **                 TAYLOR
PATCH-TO-PATCH OFFSET, RNG (M) **     0.                     PATCH-TO-PATCH OFFSET, AZ (M) **           0.
RANGE SWATH WIDTH (KM) **                 .14000000000E+01  NO OF PATCHES **                                          1
MAP START LATITUDE (DEG) **               .45000000000E+02

          * * * * * * * *   A N T E N N A   S P E C I F I C A T I O N   * * * * * * * * *
ANTENNA I.D. **                           UNITPAT            BORESIGHT NADIR AT TO (DEG) **                .20000000000E+02
BORESIGHT SQUINT AT TO (DEG) **           .90000000000E+02  AZIMUTH ANGULAR COVERAGE (DEG) **             .12800000000E+01
ELEVATION ANGULAR COVERAGE (DEG) **       .67300000000E+01  PHASE CENTER, BODY AXIS X (M) **           0.
PHASE CENTER, BODY AXIS Y (M) **      0.                     PHASE CENTER, BODY AXIS Z (M) **           0.
COORD SYS, BODY AXIS ROLL, (DEG) **   0.                     COORD SYS, BODY AXIS PITCH, (DEG) **      -.70000000000E+02
COORD SYS, BODY AXIS YAW, (DEG) **        .90000000000E+02  PLAT ROLL RATE (DEG/S) **                  0.
PLAT PITCH RATE (DEG/S) **            0.                     PLAT YAW RATE (DEG/S) **                   0.

          * * * * * * * *   T E R R A I N   S P E C I F I C A T I O N   * * * * * * * * *
TERRAIN I.D. **                           TESTPATERN         NO OF DISCRETES **                                       71
NO OF FIELDS **                                           4  TOTAL NO OF SCATTERERS **                              1095
X-AXIS COVERAGE (KM) **                   .12000000000E+01  Y-AXIS COVERAGE (KM) **                       .12000000000E+01
TERRAIN CENTER, R (KM) **                 .63675192370E+04  TERRAIN CENTER, LAT (DEG) **                  .45000000000E+02
TERRAIN CENTER, LONG (DEG) **             .34191125864E+03
```

```
       * * * * * *   S Y N T H E T I C   A R R A Y   P A R A M E T E R S   * * * * * *
SYNTHETIC ARRAY NO  **                          1 TRANSMISSION START TIME (S)  **          .78561515863E+03
ARRAY LENGTH (M)  **             .61201445587E+03 ARRAY INCLINATION (DEG)  **              .83441538944E-01
ARRAY FORMATION TIME (MS)  **    .82064825645E+02 PLATFORM VELOCITY (KM/S)  **             .74576947323E+01
NO OF PULSES  **                              900 PRF (HZ)  **                             .10970162745E+05
NO OF RANGE SAMPLES  **                       223 NO. OF AZIMUTH FILTERS  **                            223
PATCH CENTER RANGE SAMPLE NO.  **             112 SLANT RANGE SWATH WIDTH (KM)  **         .53969587071E+00
SLANT RANGE RESOLUTION (M)  **   .96374293468E+01 SLANT RANGE SAMPLE INTERVAL (M)  **      .24093573367E+01
START RANGE (KM)  **             .86821426692E+03 RANGE PATCH CENTER (KM)  **              .86848170559E+03
SQUINT ANGLE PATCH CENTER (DEG)  **  .90053327205E+02 NADIR ANGLE PATCH CENTER (DEG)  **   .20000752667E+02
LOS AZIMUTH AT PATCH CENTER (DEG) ** -.11295033230E+03 LOS INCIDENCE AT PATCH CENTER (DEG)** .22674608890E+02
PATCH CENTER, R (KM)  **         .63675192370E+04 ORBITER MASS CENTER, R (KM)  **          .71766886465E+04
PATCH CENTER, LAT (DEG)  **      .45000000000E+02 ORBITER MASS CENTER, LAT (DEG)  **       .43905755848E+02
PATCH CENTER, LONG (DEG)  **     .34191125864E+03 ORBITER MASS CENTER, LONG (DEG)  **      .33849303127E+03
PATCH CENTER PIXEL POWER IS .9999999853453

         ARRAY STATISTICS FOR  42816 POINTS.
MAXIMUM 334.4778558682,  MINIMUM 5.133558976068E-13
MEAN .1784881654176,  SIGMA 4.849835825272
EOF WRITTEN ON CIMAGE     , AFTER RECORD 224
```

PRECEDING PAGE BLANK NOT FILMED

K_u-BAND WAVELENGTH DATA

PRECEDING PAGE BLANK NOT FILMED

```
--------- PROGRAM FILTER IN EXECUTION ----------
INPUT KBRANCH                                  0
INPUT IFILIOF,IFILIMG
NPUT I/Q DATA ON IQDATF     , FILE 1
JTPUT IMAGE DATA ON CIMAGE     , FILE 10
FT SAMPLE INTERVAL IS SET AT SIA/1
O. OF FILTERS REQUIRED FOR FULL PRF COVERAGE IS 3110
RESUM RATIO OF 13 IS DERIVED FROM A SAMPLE POINT ERROR TOLERANCE OF .002
O. OF PRESUMMED FFT FILTERS IS 239
```

```
          * * * * * * * * * *   P L A N E T   S P E C I F I C A T I O N   * * * * * * * * * *
PLANET NAME  **                           EARTH             EQUATORIAL RADIUS (KM)  **                  .63781670000E+04
ECCENTRICITY  **                          .81820179996E-01  GRAVITATIONAL CONSTANT (KM3/SEC2)  **  .39860100000E+06
ROTATIONAL RATE (DEG/S)  **               .41780745995E-02  TIME OF PRIME MERIDIAN PASSAGE (S) **0.

          * * * * * * * * * *   O R B I T   S P E C I F I C A T I O N   * * * * * * * * * *
ORBIT I.D.  **                            794CIRCULR        SEMI-MAJOR AXIS (KM)  **                    .71865400000E+04
ECCENTRICITY  **                          .20000000000E-02  INCLINATION (DEG)  **                       .10800000000E+03
LONG OF ASCENDING NODE (DEG)  **       0.                   ARGUMENT OF PERIGEE (DEG)  **            0.
TIME OF PERIGEE PASSAGE (S)  **        0.                   ROTATIONAL RATE (DEG/S)  **                 .59376152657E-01
ORBITER INITIALIZATION TIME(S)  **     -.10000000000E-03

          * * * * * * * * * *   R A D A R   S P E C I F I C A T I O N   * * * * * * * * * *
RADAR I.D.  **                            SEASAT-A          OPERATING WAVELENGTH (M)  **                .18000000000E-01
RECIEVER/TRANSMITTER BW (MHZ)  **         .15553790968E+02  RANGE TIME-BANDWIDTH PRODUCT  **            .10000000000E+01
SIGNAL-TO-NOISE RATIO (DB)  **            .10000000000E+03  A/D SAMPLE RATE (MHZ)  **                   .62215163872E+02
SAMPLE LENGTH OF RANGE CORRELATION **                    1  SAMPLE LENGTH ACROSS PHASE INTERVAL *                      1
BINARY PHASE CODE  **                     B                 BINARY PHASE CODE SEQUENCE  **              RANDOM
GROUND RANGE RESOLUTION (M)  **           .25000000000E+02  AZIMUTH RESOLUTION (M)  **                  .25000000000E+02
RANGE SAMPLING RATIO (M)  **              .40000000000E+01  AZIMUTH SAMPLING RATIO (M)  **              .40000000000E+01
RANGE IMPULSE RESPONSE FUNCTION  **       COSINE**2         APERTURE WEIGHT FUNCTION  **                TAYLOR
PATCH-TO-PATCH OFFSET, RNG (M)  **     0.                   PATCH-TO-PATCH OFFSET, AZ (M)  **        0.
RANGE SWATH WIDTH (KM)  **                .14000000000E+01  NO OF PATCHES  **                                          1
MAP START LATITUDE (DEG)  **              .45000000000E+02

          * * * * * * * * *   A N T E N N A   S P E C I F I C A T I O N   * * * * * * * * *
ANTENNA I.D.  **                          UNITPAT           BORESIGHT NADIR AT TO (DEG)  **             .20000000000E+02
BORESIGHT SQUINT AT TO (DEG)  **          .90000000000E+02  AZIMUTH ANGULAR COVERAGE (DEG)  **          .12800000000E+01
ELEVATION ANGULAR COVERAGE (DEG)  **      .67300000000E+01  PHASE CENTER, BODY AXIS X (M)  **        0.
PHASE CENTER, BODY AXIS Y (M)  **      0.                   PHASE CENTER, BODY AXIS Z (M)  **        0.
COORD SYS, BODY AXIS ROLL, (DEG)  **   0.                   COORD SYS, BODY AXIS PITCH, (DEG) **     -.70000000000E+02
COORD SYS, BODY AXIS YAW, (DEG)  **       .90000000000E+02  PLAT ROLL RATE (DEG/S)  **               0.
PLAT PITCH RATE (DEG/S)  **            0.                   PLAT YAW RATE (DEG/S)  **                0.

          * * * * * * * * *   T E R R A I N   S P E C I F I C A T I O N   * * * * * * * * *
TERRAIN I.D.  **                          TESTPATERN        NO OF DISCRETES  **                                       71
NO OF FIELDS  **                                         4  TOTAL NU OF SCATTERERS  **                              1095
X-AXIS COVERAGE (KM)  **                  .12000000000E+01  Y-AXIS COVERAGE (KM)  **                    .12000000000E+01
TERRAIN CENTER, R (KM)  **                .63675192370E+04  TERRAIN CENTER, LAT (DEG)  **               .45000000000E+02
TERRAIN CENTER, LONG (DEG)  **            .34191125864E+03
```

```
****** S Y N T H E T I C   A R R A Y   P A R A M E T E R S ******
SYNTHETIC ARRAY NO **                                  1 TRANSMISSION START TIME (S) **            .78561515863E+03
ARRAY LENGTH (M) **                   .35252032658E+03 ARRAY INCLINATION (DEG) **                  .83440120929E-01
ARRAY FORMATION TIME (MS) **          .47269339572E+02 PLATFORM VELOCITY (KM/S) **                 .74576949283E+01
NO OF PULSES **                                      896 PRF (HZ) **                                .18948320562E+05
NO OF RANGE SAMPLES **                               223 NO. OF AZIMUTH FILTERS **                              223
PATCH CENTER RANGE SAMPLE NO. **                     112 SLANT RANGE SWATH WIDTH (KM) **            .53968754858E+00
SLANT RANGE RESOLUTION (M) **         .96372807317E+01 SLANT RANGE SAMPLE INTERVAL (M) **          .24093201829E+01
START RANGE (KM) **                   .86821203340E+03 RANGE PATCH CENTER (KM) **                  .86847946794E+03
SQUINT ANGLE PATCH CENTER (DEG) **    .90030717022E+02 NADIR ANGLE PATCH CENTER (DEG) **           .20000431623E+02
LOS AZIMUTH AT PATCH CENTER (DEG) ** -.11297301759E+03 LOS INCIDENCE AT PATCH CENTER (DEG)**       .22674239759E+02
PATCH CENTER, R (KM) **               .63675192370E+04 ORBITER MASS CENTER, R (KM) **              .71766884575E+04
PATCH CENTER, LAT (DEG) **            .45000000000E+02 ORBITER MASS CENTER, LAT (DEG) **            .43904820114E+02
PATCH CENTER, LONG (DEG) **           .34191125864E+03 ORBITER MASS CENTER, LONG (DEG) **           .33849372059E+03
PATCH CENTER PIXEL POWER IS .9999999942407

         ARRAY STATISTICS FOR  42816 POINTS.
MAXIMUM 342.3376838039,  MINIMUM 8.954632127766E-15
MEAN .1809995086503,  SIGMA 4.959671117744
EOF WRITTEN ON CIMAGE     , AFTER RECORD 224
```